Seafloor characterization using keel-mounted sidescan: proper compensation for radiometric and geometric distortion.

John E. Hughes Clarke
Ocean Mapping Group, Dept. Geodesy and Geomatics Engineering, University of New Brunswick

Abstract

Keel- mounted sidescan staves represent an efficient method of maintaining near-100% seafloor ensonification, even in very shallow (<10m) coastal waters, as the swath width is defined by slant range rather than angular sector. Unlike towed sidescan systems, however, the aspect ratio varies strongly as the arrays are held fixed relative to the surface. As a result, the geometry of shadow casting, so critical in qualitative sidescan interpretation can vary rapidly providing apparent changes in the sidescan textural context that are unrelated to seafloor change.

As the sidescan is rigidly mounted to the vessel, it suffers from the more pronounced yawing and rolling experienced by the surface vessel. At this time, the sidescan system deployed does not integrate orientation information. Therefore, that information from a simultaneous MBES system is used to provide improved geometric control. Particular problems include time synchronization between the MBES (locked to GPS time) and the sidescan clock (independent and with a drift). The use of high quality yaw can significantly improve target location but reveal the distortion of the scanning pattern making both mosaicing and spatial texture analysis more complicated. The roll information is critical in the proper correction for radiometric effects particularly if the backscatter angular response is needed.

An automated method for extracting and mapping spatial frequency information from the corrected sidescan backscatter data is presented. By combining a number of discrete spatial frequency bins together with the corrected average backscatter strength, improved seabed classification is possible. Example data from a large scale (30 day) shallow water (av. depth 4m) survey in Shippagan Bay is used to illustrate the practical implementation, problems and potential for seafloor characterization.

Introduction

Because a disproportionate percentage of human activity occurs in the immediate coastal zone, environmental surveys are being increasingly focused in extremely shallow water depths (<5m at times) that provide practical operational difficulties in sonar deployment. Geometrically, in depths less than 10m, it is hard to justify 100% swath bathymetry unless the area is a critical shipping lane. Where bathymetric information is the only requirement, either the old model of single beam profiling or now the more dense laser bathymetry is being most commonly used.

Yet if the requirement is for seabed classification, whilst single beam solutions do exist (Heald et al., 1999) they reflect incomplete coverage and lidar backscatter is not yet a well understood and robust seabed classifier. Amongst geoscientists, qualitative analysis of sidescan imagery is favoured . Such analysis has a number of complications however:

- Third party users such as biologists are less comfortable with subjective classifications (what exactly does fuzzy and speckled mean?).
- Geometrically it is actually quite difficult to deploy sidescans in such shallow waters.
- Sidescan classfication/segmentation algorithms, whilst not new are not well trusted.

One approach to overcoming the geometrical difficulties with conventional towed sidescan, is actually to return to the early development of the system and use fixed mounts. This avoids the propeller wash issue and is a lot kinder to the hardware. Herein that model has been adopted to address coastal habitat mapping, but a number of constraining factors operationally complicate the acquisition and analysis.

Instrumentation

The hardware used herein involves Knudsen 320 dual channel echo sounders employing twin 200 kHz channels driving Airmar sidescan staves. This approach has the advantage of being able to use existing conventional single-beam digital signal processing units common throughout the Canadian Hydrographic Service and makes use of low priced sidescan staves adequate for the needs of this program.

Two Airmar 200 kHz, 0.5° by 50° staves have been mounted along the keel of a semi-displacement hydrographic survey launch (C.S.L. Heron , a 34 ft CHS standard H boat). The arrays are tilted down by 30° from the vertical and mounted on the skeg at a depth of ~ 80cm below the waterline.

The staves are driven by a Knudsen 320M (using a PC control package, with the analog display unit disabled), logging the 16 bit binary echo envelope through a SCSI interface. The absolute source level of each array is unknown but there are 8 relative power levels whose relative level has been estimated. Gated continuous wave (CW) pulses in the range 0.05 to 2.0ms are available. The system can alternately be configured using a chirped pulse with up to 4ms pulse length but this was not employed herein. The data are logged using a 40log R gain ramp with a range of fixed gain offsets (again relative steps have been empirically estimated). The digitized data is really 12 bit, stored in a 16 bit field for convenience. The data is logged as a voltage proportional to linear amplitude.

The 320M is interfaced only to a single serial GGA position input. The sonar clock is set manually on a daily basis. The internal clock is known to drift pseudo-randomly several seconds over the course of the day. The 320M can accept a heave input from a telegram that contain pitch, roll and heave, but that data format was incompatible with that

required by the multibeam and as of end 2003, the Knudsen did not parse or use the roll, pitch or heading information anyway.

On the same platform, there is a Simrad EM3000S multibeam sonar integrated with an Octopus F-180 motion sensor (with a Seatex MRU-6 as an on-line backup). This system receives the identical GGA string and the clock is continually reset to within 10ms of UTC time using a combination of ZDA strings and the 1PPS signal. The data thus represents a source of information about a subset of the across-track topography, but most particular if the clocks offsets can be resolved (as the two systems receive the identical position solutions), also represents a source of information about yaw, pitch, heave and heading. The clock drift was estimated separately for each survey line by averaging all of the instantaneous time offsets for each common fix within that single file and using that average as the time latency between the two sonar clocks.

Data Acquisition

Data for this analysis were acquired as part of a 30 day deployment to Shippagan Bay and approaches in Northern New Brunswick. The depths in the area range from 2 –20m averaging typically 4-6m. The main aim of the survey was to characterize the diversity in seabed habitat as part of a DFO study of the impact of fisheries (lobster, mackerel, herring) aquaculture (mussels and oysters) and fish plant activity (Duxfield et al., 2004). The data were acquired from C.S.L Heron at speeds of 7-8 knots in seastates less than 3.

Shippagan Bay *(1km grid graticules)*
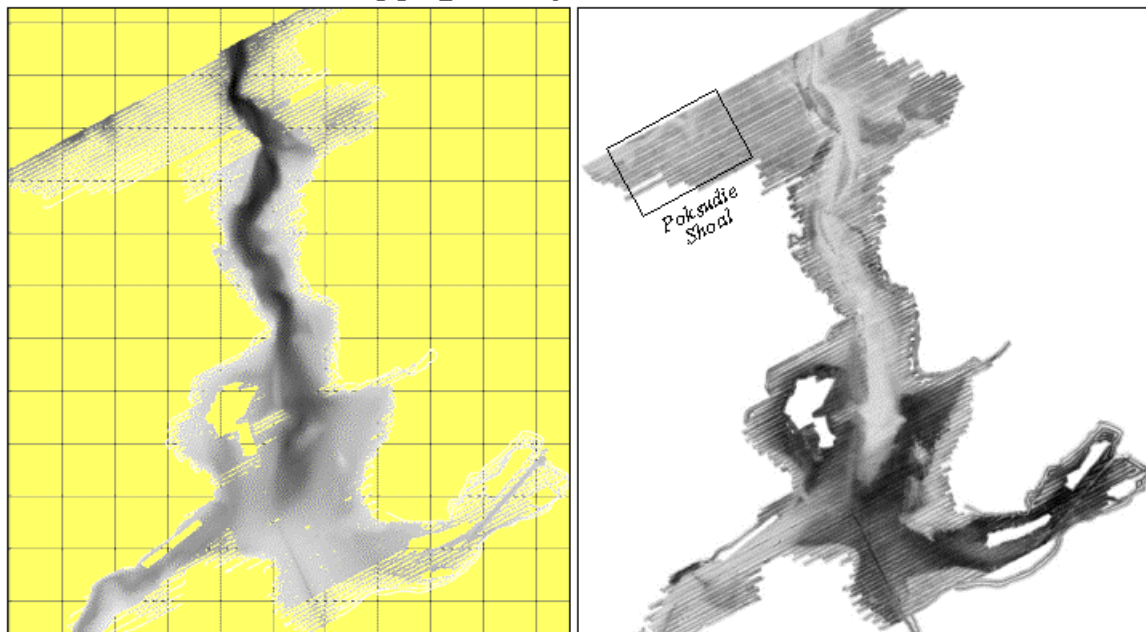
| A: multibeam bathymetry | B: 200 kHz sidescan mosaic |
| *(0-20m range)* | *(greyscale – 30dB dynamic range)* |

Figure 1: regional bathymetry and mean backscatter strength image of Shippagan Bay showing location of focus area on Pokesudie Shoal (enlarged in Figure 9).

Data Manipulation

The aim of the data reduction was to examine the spatial and angular variations in bottom backscatter strength. As the absolute source level and receiver gain sensitivity levels are unknown, the aim was to come up with a robust measure of relative changes in backscatter strength.

Propagation

The system already provides a 40 logR gain ramp to account for spherical spreading. This was combined with attenuation of ~ 50 dB per km (200 kHz, 10 ºC, 32 ppt). Finally, based on the slant range, the known pulse length of 0.1ms (7.5cm slant range equivalent), the nadir altitude (and using a flat seafloor correction), and the assumed beam width of 0.5º an estimate of the instantaneously ensonified area was calculated in the manner described by Mitchell and Somers (1989).

Radiation Pattern

The most visible residual signature is that of the product of the transmit and receive beam patterns. The arrays are designed to have a 50º beam width in elevation. The specific beam patterns were however unknown and the mount angles were not precisely machined. Furthermore, as the arrays sit in a concave section of the keel there is a viable probability that reflections off the surrounding hull might influence the angular sensitivity.

As a result, an empirical approach was employed to estimate the net sum of radiation and reception beam patterns (inescapably mixed with the mean seabed backscatter angular response). Using the instantaneous roll at transmit for the <0.1 second ping interval the orientation was assumed to be constant, (a reasonable approximation as the roll rates were low and the roll timing synchronization was questionable anyway). The method used was to stack backscatter strength information in angular bins referenced to the sonar reference frame.
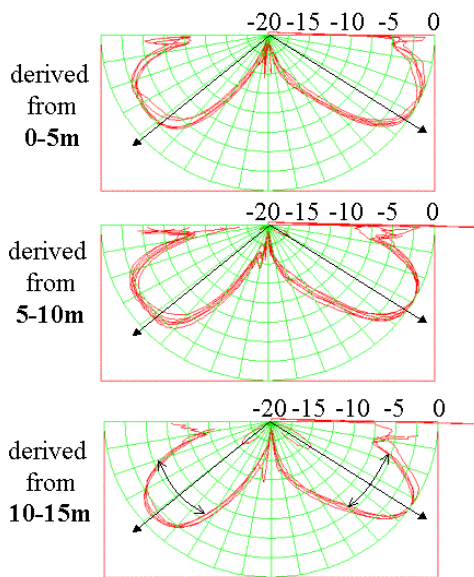
Empirically derived pseudo-beam patterns
Representing product of transmit and receive
beam patterns and mean seafloor angular response.

Figure 2: showing stacked relative backscatter strength data compiled for each day for 10 survey days. The data are used as an empirical estimate of the transducer beam pattern product. They were compiled in the sonar-reference frame allowing for instantaneous roll. Data collected within 5 degrees of the local level was excluded and information on the beam pattern at lower grazing angles was obtained when that side was rolled down.

Data are presented referenced to the peak sensitivity axis. As this represents the product of the transmit and receive beam patterns, the –6 dB level represents the best estimate of the transducer beam width. Interestingly the beam width appears closer to 38º than the manufacturers nominal design of 50º

Example estimates of the combined radiation and seabed backscatter strength pattern are shown (Fig. 2). It was apparent that, even after correction for attenuation and ensonified area, there appeared to be a strong dependence on this pattern at low grazing angles as a function of water depth. Two reasons are considered for this. The first is that the sediments in Shippagan bay are strongly correlated with depth. Depths greater than 10m almost exclusively include the floor of the current swept channels where high backscatter sediment dominate. Inversely, the shallower sediment tend to occur in areas of lower current. And in the shallowest regions wave action and eelgrass growth provide a unique scattering environment. It is highly probably that the distinct sediment types have significantly different shapes to their backscatter strength angular response that, of course is overprinted on top the mean angular signature. The second issue is that with the extreme aspect ratios seen in very shallow water, the data beyond ~ 70º is probably significantly contaminated with surface clutter artificially raising the apparent signal strength at extremely low grazing angles (fig. 3).
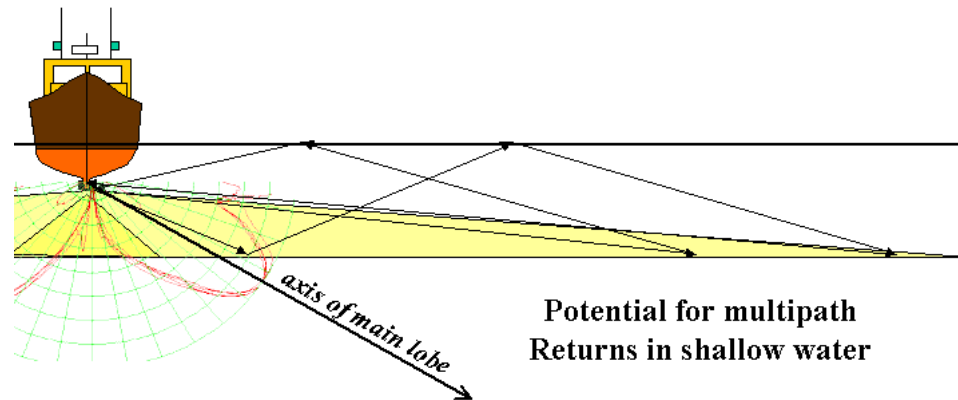
Figure 3: surface clutter issues contaminating the beam pattern estimates at extremely low grazing angles in shallow water.

Sensitivity to estimate of sonar altitude.

Bottom tracking, based on the received echo time series, from these Knudsen staves proved difficult due to the common presence of water column noise and the low receiver sensitivity close to normal incidence. By using the EM3000 bottom tracking distance (strictly the absolute two way travel time, not heave corrected and adjusted for the lever arm from the EM3000 to sidescan transducers) we could significant improve this. The best approach was found to be to use a slightly filtered version of the minimum slant range measured by the EM3000.

Validity of extremely low grazing angle estimates

It depths less than 3m, the aspect ratio in the outer swath was 1 in 25 (2.3º off horizontal) or lower. Under these extreme geometries, one has to consider whether it valid to expect data collected at these low grazing angles to be predominantly controlled simply by radiation geometry and not include sea surface or multiple contributions (eg. Fig 3). This contamination is clearly suggested by the apparent increase in the radiation levels at lowest grazing angles seen in the shallower water beam patterns (Fig. 2).

One approach to avoiding this was to only use data at higher aspect ratios, relying on the vessel to roll to down on that side so that one can examine the real radiation pattern at those extreme angles w.r.t. the array. This worked reasonably well for the data acquired in depths > 10m. But those beam pattern estimates cannot be used for the shallow water data as they underestimate the radiation at those lowest grazing angles. As a result the apparent backscatter strength actually increased at the lowest grazing angles, producing a striped aspect to the sidescan mosaic (Fig 1, right).

Visual impact of radiation pattern corrections.

It was very apparent when the hull was undergoing rapid rotations, as striping would appear in the image. In principle this should be efficiently alleviated by proper application of the empirically estimated radiation patterns.
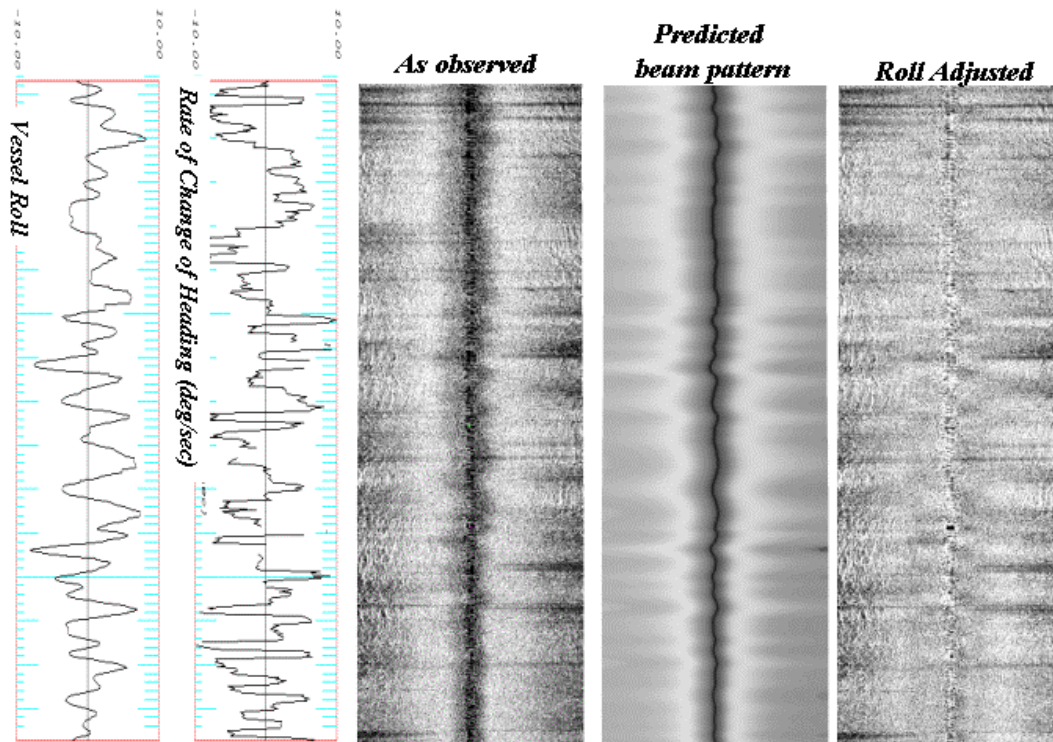
Figure 4: beam pattern correction attempts. The null close to nadir is reasonably predicted, but the compensation outboard of the boresite is poor, presumably due to other effects including yaw rate, bubble noise and surface clutter. (vessel steaming down the page)

Examples are shown (Fig. 4) where this was the attempted where it worked well in the near nadir regions. In deeper water where radiation patterns shallow than 10 degrees off level were not used the results are encouraging. But in v. shallow water, gross artifacts were often introduced that looked worse than the original data. This would appear to indicate that the influence of surface clutter (presumably mainly roll independent) is overprinting the data and thus cannot be removed in the same manner.
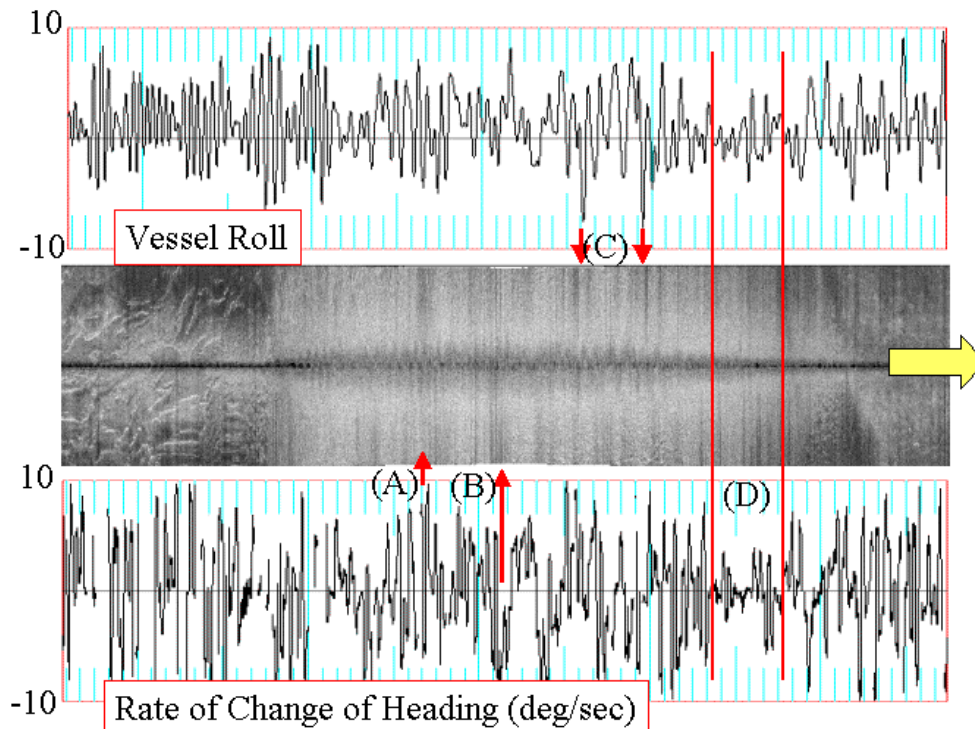
Figure 5: showing periods where roll and yaw rates correlate with striping in the data.
   A: period of high +ve yaw (turning to right) producing striping on port side
   B: period of high –ve yaw rate (turning to left) producing striping on stbd. side
   C: two periods of high –ve roll (stbd. up) producing low backscatter on port side
   D: period of weak roll and yaw yet still intense striping

An addition problem may well be a result of the high yaw rates. With 0.5º beams, yaw rates in excess of 10º per second could result in completely non-overlapping transmit and receive beam patterns for one side. Visual correlation of yaw rates shown against banding in the data (Fig. 5, A and B), indicate that yawing was an additional contribution that may overprint the more obvious roll induced striping (Fig. 5 C). Because the sidescans are fixed to the keel, all the helmsmans efforts to maintain the line translate into high yaw rates.

Attempts to minimize the result of roll and yaw rates were only marginally successful however. Part of this may be that under those conditions, there were often breaking waves and much of the signal attenuation has more to do with bubbles in the near surface waters than instantaneous orientation. Figure 5D shows a period when the striping is present even whilst the vessel is relatively stable.

Derivation of Backscatter Strength Estimates

Ideally an estimate of backscatter strength as a function of grazing angle may be used as a classifier (e.g.: Hughes Clarke et al., 1997). In practice, because the prediction of first arrival was so poor (in part due to the deliberately weak part of the beam pattern at that elevation angle) and the pulse length effectively smears this zone, data within ~ 30º degrees of vertical incidence are not usable. And beyond ~70º the sea-surface clutter appear to contaminate the useful data.

Furthermore, however, the method of empirical beam pattern estimation unavoidably includes the mean seabed angular response shape in the stacked response with angle. Therefore the data, (which is already relative), can only provide relative changes on the shape of the angular response curves. Even with these limitations it is apparent that mean backscatter strength is an incredibly powerful classifier. Clearly coherent zones of common mean backscatter strength can be seen (Fig 1). Nevertheless the mean backscatter strength image is prone to artifacts. Most notably, in shallow water areas where there are significant sea surface contributions, one can see swath parallel banding that are obviously not a result of natural seabed geological variations. Thus one seeks other means of classifying the data.

Derivation of Spatial Texture Parameters.

Given that the of measure backscatter strength alone is an imperfect indicator of seabed type a natural second order classifier to turn to is spatial texture. Qualitative interpretation of sidescan texture is well established (Somers and Stubbs, 1984). Experienced marine geologists have long interpreted seabed type based on textural patterns (for example, commonly the appearance of bedforms, bedrock or boulders) in the image. These textures are recognizable even in the presence of imperfect geometric, radiometric or propagation data reduction (for example automatic gain controls). To take this classification further however, one needs to be able to separate regions that have more subtle textural variations, not immediately identifiable as a specific sediment type.

There is an extensive set of literature on automated sidescan texture classification (Blondell and Murton, 1997 and references therein). Two different approaches are common. Some algorithms work on the raw intensity time series data (i.e. effectively 1D) and are thus azimuth specific (Reut, et al., 1985; Pace and Gao, 1988). Others work on the 2D spatial texture either along the imaging corridor (i.e. in slant range and alongtrack coordinates, e.g. Pace and Dyer, 1979)) or in the final georeferenced mosaic (Reed and Hussong, 1989).

Grazing Angle Variation across the swath

altitude (m)	across track distance (m)				
	10	20	30	40	50
1	84.3	87.1	88.1	88.6	88.9
2	78.7	84.3	86.2	87.1	87.7
5	63.4	76.0	80.5	82.9	84.3
10	45.0	63.4	71.6	76.0	78.7
15	33.7	53.1	63.4	69.4	73.3

Figure 6: Illustrating the variation in grazing angle as a function of horizontal range for the depths encountered in this survey.

The first approach is unavoidably sensitive to azimuth but also grazing angle. However for a typical sidescan that assumes a near constant aspect ratio (i.e. towed at a constant

altitude), the central part of the echo trace has little grazing angle variations (see table above, Fig 6)). For high aspect ratio systems and especially those fixed to the surface, grazing angle variations cannot be ignored. The classic Pace and Gao (1988) spectral analysis approach looks strictly at a time series rather than a range series. For low aspect ratio sidescans the two are closely correlated. This is not the case for high aspect ratio systems and these keel mounted sidescans vary between the two geometries as the depth changes.

The Pace and Gao approach examines the shape of the power spectrum from a sidescan time series. This is nearly equivalent to looking at the spatial frequency content of the radial component of backscatter strength variability. For low aspect ratio systems treating slant range and horizontal range scales as equivalent is an acceptable approximation.

Azimuthal sensitivity.
 Because the radial and azimuthal sampling patterns are quite different, interpretation of spatial texture has to proceed with caution. Radially one is constrained by range resolution whereas in the azimuth direction one is constrained by along track sampling and beam width. For terrains with a strong azimuthal heterogeneity, imaging direction is important. The classic example is sand waves. And thus if only radial spatial statistics are considered then the same seabed may be classified differently at different azimuths. The nature of sidescan imaging however, with the topographic component of the signal being itself dependent on azimuth, makes this hard to avoid anyway.
One particular advantage of considering radial variations only is that it significantly lowers the sensitivity of the classification to striping or other along-track signal fluctuations that are a result of imaging geometry rather than the seabed. A particularly pronounced example is the roll and yaw driven striping (Fig. 5) seen in the data herein.

For the Pace and Gao approach, the spectra were normalized so that only the relative shape of the spectra were examined. In the case described herein, because changes in the pulse length, source level and receiver gains have been tracked we now have the advantage of being able to use the absolute spectral power estimates as an extra degree of freedom.
At the shortest spatial wavelengths one is examining both the spatial texture and the speckle character. Speckle character can be examined through probability distribution functions (deMoustier 1986, Stewart et al., 1994) to try and characterize the relative contribution of coherent and incoherent scattering. For CW systems, the pulse length will limit the shortest spatial wavelengths at which speckle is important.

For wavelengths larger than the physical pulse length, one can start to examine true spatial variability. Physically this can be interpreted as seabed "patchiness". Variations in seabed backscatter strength over wavelengths of metres can be the result of several aspects including: shadowing due to topography, spatial changes in seabed surface roughness and/or impedance (e.g. grainsize or perhaps algal growth), spatial changes in shallow seabed volume scattering (variations in burrow density). As we do not have

control of the off-track topography we cannot rigorously separate topographic from surface textural variations.

In the absence of clear identifiable signatures like bedforms or bedrock, much of sidescan texture is hard to attribute to physical character. Video tow data, if available can indicate patchiness. Nevertheless we now have an extra degree of freedom to exploit. Areas of identical swath-averaged mean backscatter strength may have different spatial texture characteristics.

To reveal these degrees of freedom, a derivation of the original Pace and Gao classifier has been implemented on the Knudsen sidescan (Fig. 7). For three 12.8m seafloor sections in width: one in the center of the swath on either side, a patch approximately equal to a square on the seafloor (with a ping rate of 6Hz and 2.5-3.5m/s this is equivalent to ~24 to 30 pings). The data is actually resampled to a fixed horizontal range to account for the high aspect ratios seen with the keel-mounted geometry. The data is examined at 0.1m horizontal range resolution (slightly larger than to the range resolution justified by the pulse (~8 cm except at large grazing angles)). Power spectra are derived for each of these sections for the 24-30 pings. Prior to deriving the spectra, each section is detrended and a hamming window used to taper the section ends. The spectra are derived from logarithimic intensity data corrected for beam pattern and ensonified area as described above. These data are thus effectively measures of the relative backscatter strength. The average spectra (derived bv stacking the 32 individual spectra) for that patch is then used as a classifier.
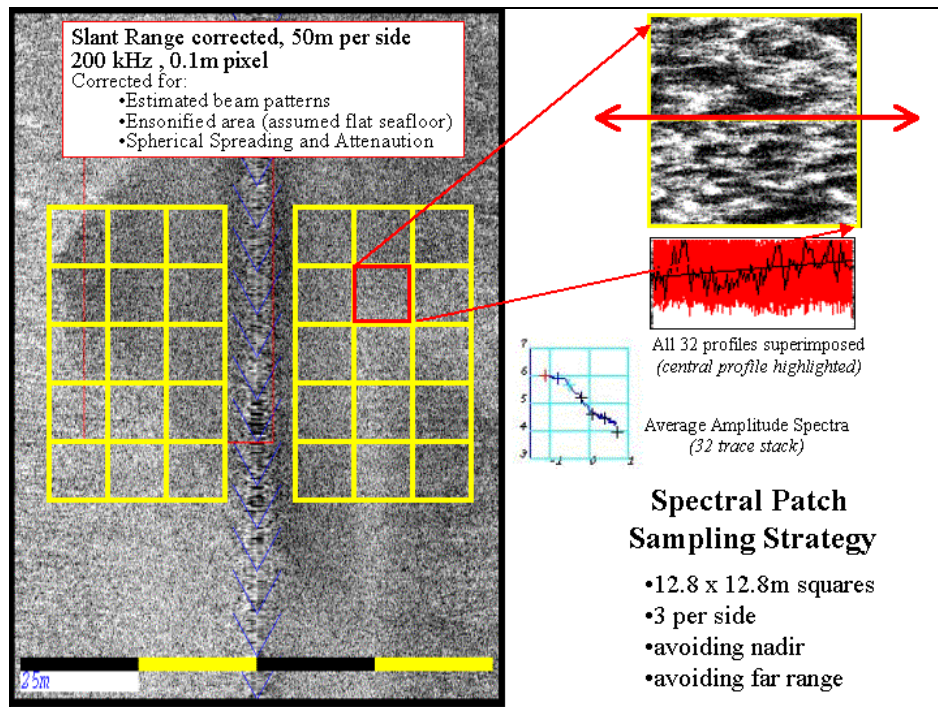
Figure 7: showing sampling strategy for extracting spectral properties.

Ratios of different sections of the spectrum have been previously used to try and come up with useful classifiers (Pace and Gao, 1988). The reason for using ratios, was that for most previous studies, the absolute magnitude of the spectra was not useful as the systems usually had automatic (or undocumented manual) gain controls. In this case, we have stable relative spectral levels and thus we may examine the total power within narrow spectral wavelengths. A previously developed graphical tool (jview -sslook) was used for examining full resolution sidescan trace data in a geographic context. A new addition has been developed allowing the user to directly visualize the spectrum of radial spatial wavelengths for any piece of sidescan.

From that spectrum the energy density at 7 specifics spatial wavelengths has been extracted to uses as metrics for analysis. The wavelengths chosen were : 12.8, 6.4, 3.2, 1.6, 0.8, 0.4 and 0.2 metres. Ultimately these metrics may be combined with mean backscatter strength and other quantiles. Other authors have looked at metrics such as variance, kurtosis and skewness. These however have to be derived from a finite area and thus in the presence of patchiness (common in shallow water environments) have a spatial wavelength dependence in themselves.

For the purposes of this paper, the spectral power densities within each narrow band are presented as geographic maps so that a visual correlation between the differences in their spatial distribution may be examine and compared with imagery itself (Fig. 8).
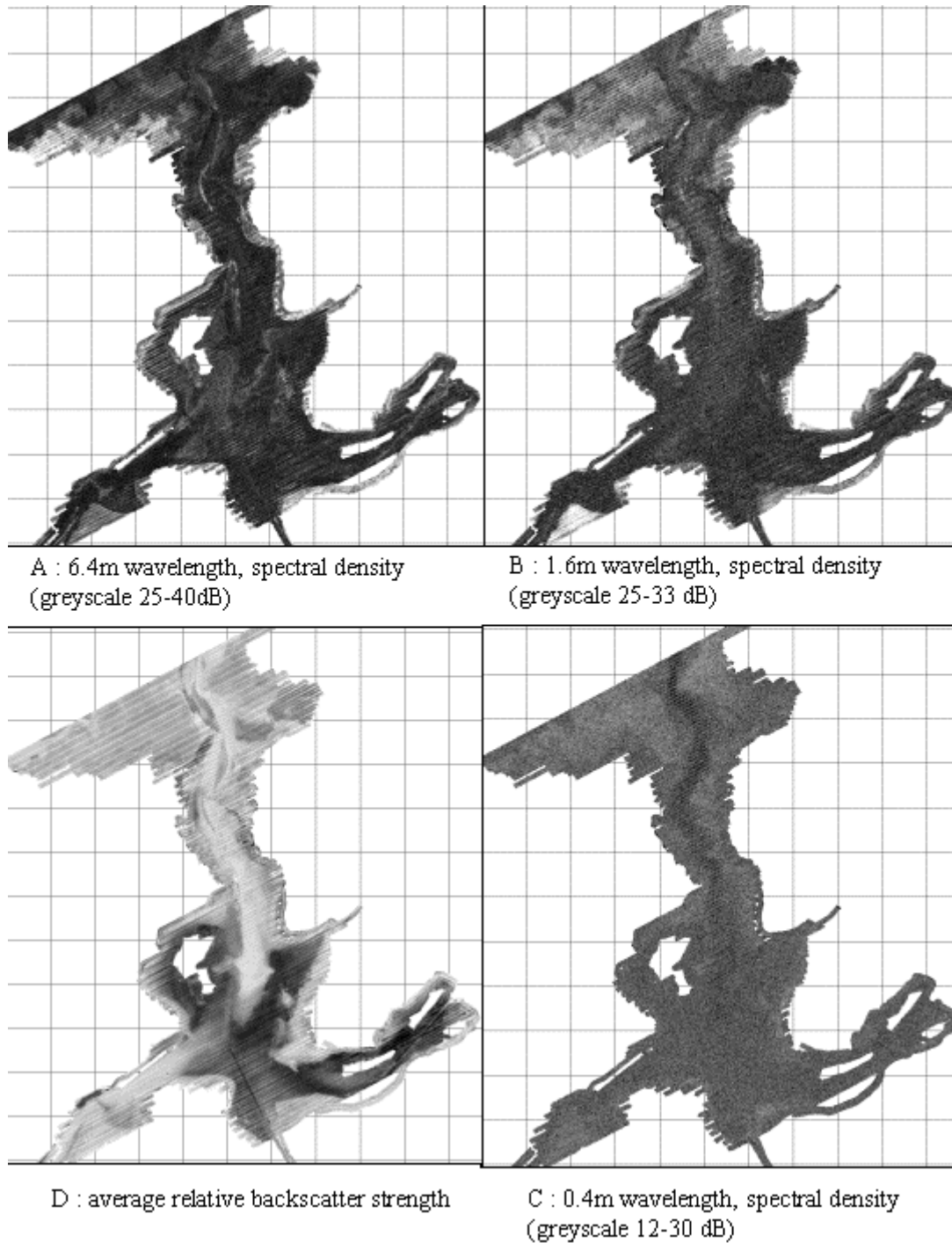
Figure 8: spatial distribution of average relative backscatter strength (D) and three representative spatial wavelengths.

A significant depth dependence was observed at the shortest spatial wavelengths (Fig. 8C). This is probably due to resampling to ground range. Because of the higher aspect ratio in deeper water, the slant range resolution translates into poorer and poorer horizontal range resolution and this impacts on the spectral content of a horizontal range series. Within the 40cm band and especially the 20cm band most of the signature in the

image is highly depth correlated. In the deeper water, significantly less energy is seen with a minima close to nadir where the resampling is effectively smearing out the signature reducing the short wavelength energy.

8 characteristic different types of seafloor from an area with high spatial diversity in spectral properties were selected. The area, (Pokesudie Shoal, box in Fig. 1) ranges in depth from 1-3 metres below the transducers. The 8 locations are superimposed on the sidescan mosaic of the area in Figure 9.
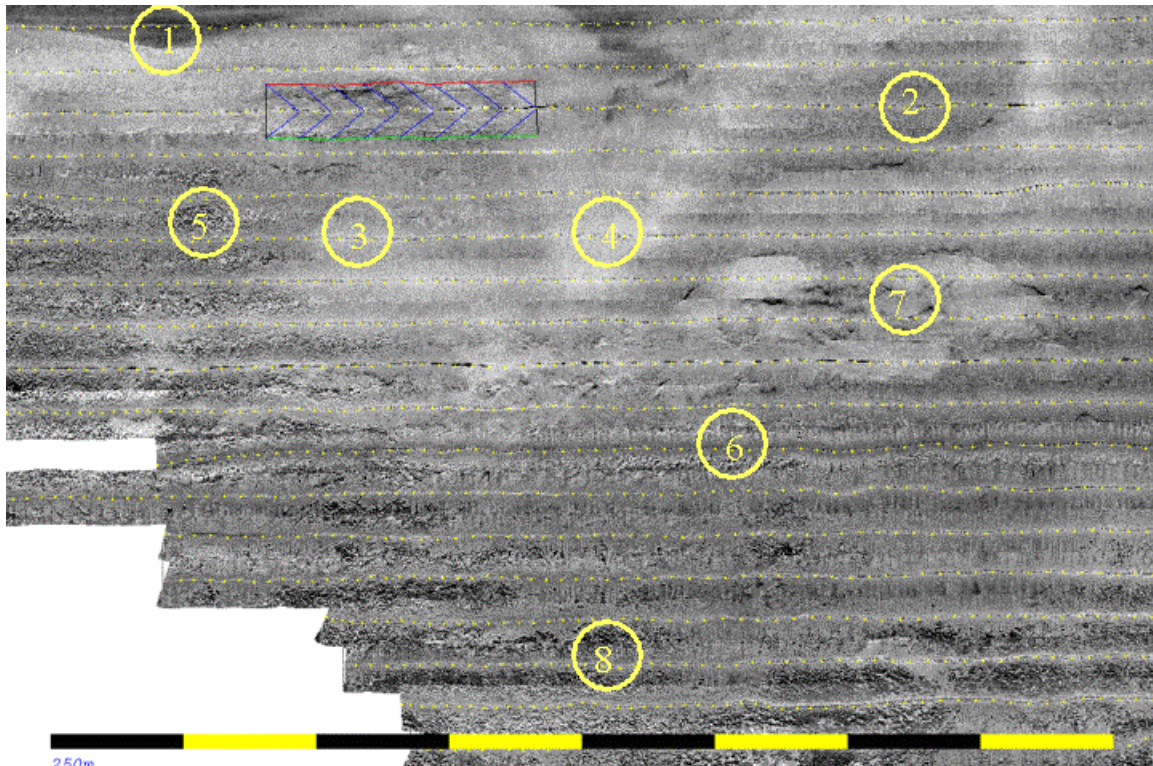
Figure 9: sidescan mosaic of Pokesudie Shoal showing the location of the eight chosen sample locations.

For each sample location an area of 25m in width and 50 m in along track dimension is presented in Figure 10 with the corresponding spectra derived from the central part of the image.
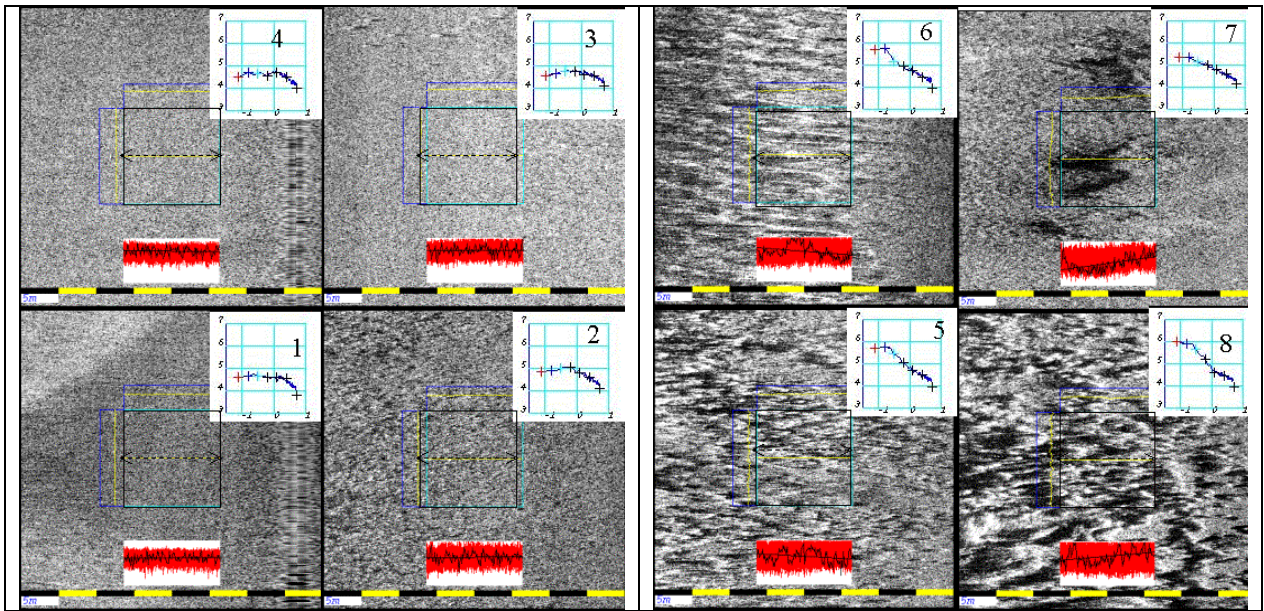
Figure 10: 8 snippets of sidescan imagery (location shown in Figure 9) with their corresponding spectrums.

Sites 1-4 were selected based on the fact that they all had little visually discernable textural signature. Whilst each area has a distinct mean backscatter strength, little separates their spectral content. Site 2 has a slightly higher energy level at 1.6m wavelength. These 4 areas would thus probably be indistinguishable from texture alone.

In contrast sites 5-8 were chosen for their strong textural characteristics. Sites 5 and 8 are differing degrees of a distinctive patchy texture developed in shallow depths that is inferred (although not proven at this time) to represent eelgrass beds. Site 7, based on multibeam bathymetry is inferred to represent shallow outcrop scarps. Site 6 in unique in that it represents texture due to the presence of a thermocline.

 Site 6 is selected from a line run several days later than the main survey (an infill line). At that time the water column conditions were significantly different, generating an overprinting texture unrelated to the underlying seabed. Colder saltier water intrudes into Shippagan Bay under certain combined tidal and wind conditions. This creates strong velocity gradients in the upper few metres. Unlike towed sidescan, the keel –mounted systems must always image through the surface sound speed stratification. Data collected under these conditions was found to be extremely misleading for classification purposes.

Looking at a range of spectra (Fig. 11) it is clear that there is little separation between the spectral power levels at wavelengths shorter than 80cm. The greatest variability is seen at the longest wavelengths. The same results were observed by Pace and Gao (1988) who based their classification on ratio of spectral energy at longer wavelengths referenced to the signal level at the Nyquist wavelength (the 0.2m band in this case).
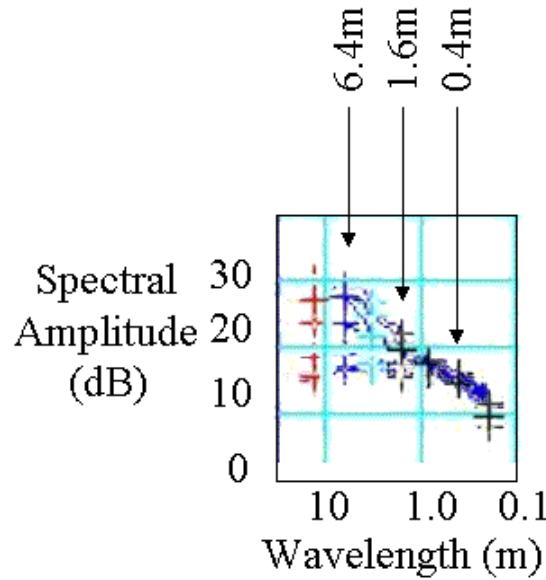
Figure 11: the eight spectra from figure 10 superimposed show the greatest variability at the longest wavelengths.

The fact that all the spectra are nearly identical at wavelengths shorter that 0.8m suggests that increasing the pulse length by up to a factor of 4 would not significantly change the spectral content of the image. This provides more freedom in operating conditions. In contrast single beam vertical incidence classification schemes are tremendously sensitive to pulse length (as, at normal incidence it controls the time-evolution of the ensonified area and thus the shape of the echo-envelope).

6.4m wavelength   1.6m wavelength
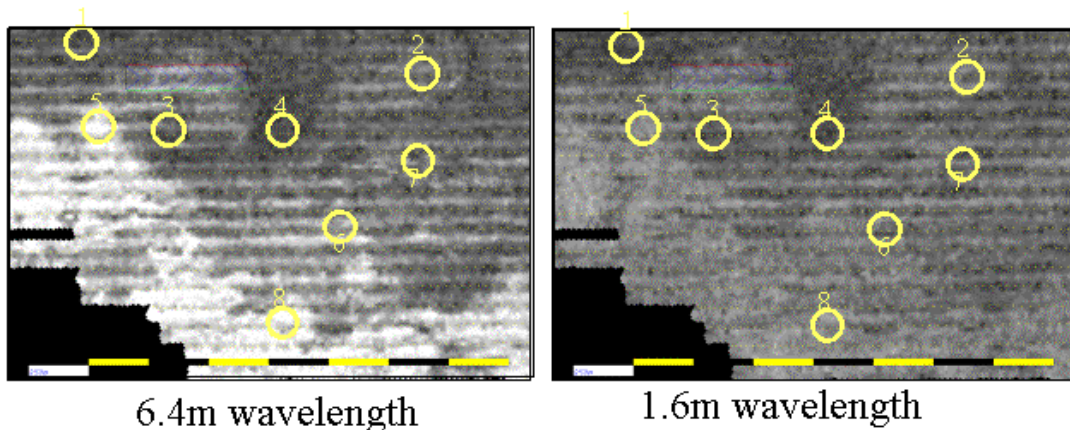
Figure 12: showing the same area as figure 9 but illustrating the variation on the 6.4m and 1.6m bands.

In Figure 12 one can see that the inferred eelgrass texture (refer to Fig. 9 to see the texture in the sidescan) shows up distinctly as anomalous high energy in the 6.4m band. Note particularly location 6 though which was the line collected in the presence of a strong thermocline. Due to the artificial patchiness induced by the watercolum, a distinct

band of anomalous high power extends along that survey line illustrating the sensitivity of the classification method to water column conditions.

Conclusions

Keel-mounted sidescans represent an economic means of deriving estimates of mean and spatial texture variation in seabed backscatter strength in extremely shallow water. In order to minimize radiometric and geometric distortions, relative power and gain level settings, empirical beam patterns estimates and full orientation information are needed to come up with a stable measure of relative seabed backscatter strength.

Using this information, one can map spatial variations in mean backscatter strength together with spectral energy in narrow bands of spatial wavelength. It was found that the textural information in the 6.4, 1,6, and 0.4m spatial wavelength ranges provides significant additional discrimination potential. Such quantitative measures may be applied regionally to come up with the underlying metric for attempting an objective approach to seabed habitat characterization.

By attributing spectral characteristics to seafloor patchiness at easily understandable spatial wavelengths, the metrics derived herein may be compared to video transect imagery. Video transect interpretation is subjective and provides no absolute measure of grain size or sound speed, density or interface roughness, which physical bottom sampling or stereo photography can. But by running a transect, spatial variability can be viewed which is lost in the more sparse bottom sampling approach.

It still remains debatable whether an objective approach such as the one described here is in any way superior to the subjective interpretation of an experienced marine geologist. A number of the limitation were recognized in this study, such as yaw-induced striping, bubble wash down, steaming through ship wakes and sea-surface and thermocline signatures which would normally be transparent to the experienced human interpreter, yet confound the objective algorithms. The objective approach however is clearly less prone to the subjectivity of individual interpreters and of course senility.

Acknowledgments

References

Ph. Blondel, B.J. Murton; 1997, "Handbook of Seafloor Sonar Imagery", PRAXIS-Wiley & Sons, 314 pp., ISBN number 0471962171, 314 pp.

DeMoustier, C., 1986, Beyond bathymetry: mapping acoustic backscatter from the deep seafloor with SeaBeam: JASA, v.79(2), p.316-331.

Duxfield, A., Hughes Clarke, J.E., Martin, B-A, Legault, J, Comeau, M. and Monahan, D., 2004, Combining multiple sensors on a single platform to meet multi-purpose nearshore mapping requirements: Canadian Hydrographic Conference, Ottawa May 2004, Conference CDROM.

Heald GJ, Pace NG, Dyer CM, 1999, ' A theoretical and experimental examination of seabed discrimination using the first and second backscatter from an echo sounder *J.Acoust.Soc.Amer*, v. 105, p.1205 .

Hughes Clarke, J.E., Danforth, B.W. and Valentine, P., 1997, Areal Seabed Classification using Backscatter Angular Response at 95 kHz: NATO SACLANTCEN Conference Proceedings Series CP-45, High Frequency Acoustics in Shallow Water, p.243-250.

Mitchell, N. C., and Somers, M. L., 1989, Quantitative backscatter measurements with a long-range side-scan sonar. IEEE J. Oceanic Engineering, v. 14, p. 368-374.

N. G. Pace and C. M. Dyer, 1979, Machine classification of sedimentary sea bottoms, *IEEE Trans. Geosci. Remote Sensing* GE-17, p. 52–56.

N.G.Pace and H.Gao, 1988, 'Swathe seabed classification', *I.E.E.E. Oceanic Engineering* 13, pp.83-90.

Reed, T.,B, IV and Hussong, D., 1989, Digital image processing techniques for enhancement and classification of SeaMARC II side scan sonar imagery: Journal of Geophysical Research, v.94, p.7469-7490.

Reut, Z., Pace, N.G. and Heaton, M.J.P., 1985. Computer Classification of Seabeds by Sonar. Nature, v. 314, pp. 426-428.

Somers, M.L., and Stubbs, A.R., 1984, Sidescan Sonar, IEE Proceedings, vol. 131, pp. 243-256.

W. K. Stewart, et. al.,, 1994, Quantitative seafloor characterization using a bathymetric sidescan sonar: *IEEE J. Oceanic Eng.* 19(4), p. 599-610.

Tamsett, D. 1993. Seabed Characterization and Classification from Power Spectra of Side-scan Sonar Data. Marine Geophysical Researches, v. 15, pp. 43-64.